Liquid Crystals

Publication details, including instructions for authors and subscription information:
http://www.informaworld.com/smpp/title~content=t713926090

Crystal structure of a mesogenic copper(II) square-planar complex bis[*N*-*p*-(*n*-Hexyloxy)phenyl, *p*-(*n*-heptyloxy)salicylaldiminato] copper(II)

A. Roviello[a]; A. Sirigu[a]; P. Iannelli[b]; A. Immirzi[b]
[a] Dipartimento di Chimica, Università di Napoli, Napoli, Italy [b] Dipartimento di Fisica, Università di Salerno, Salerno, Italy

To cite this Article Roviello, A. , Sirigu, A. , Iannelli, P. and Immirzi, A.(1988) 'Crystal structure of a mesogenic copper(II) square-planar complex bis[*N*-*p*-(*n*-Hexyloxy)phenyl, *p*-(*n*-heptyloxy)salicylaldiminato] copper(II)', Liquid Crystals, 3: 1, 115 — 122

To link to this Article: DOI: 10.1080/02678298808086354

URL: http://dx.doi.org/10.1080/02678298808086354

LIQUID CRYSTALS, 1988, VOL. 3, NO. 1, 115–122

Crystal structure of a mesogenic copper(II) square–planar complex bis[*N*-*p*-(*n*-Hexyloxy)phenyl, *p*-(*n*-heptyloxy)salicylaldiminato] copper(II)

by A. ROVIELLO and A. SIRIGU
Dipartimento di Chimica, Università di Napoli, Via Mezzocannone 4, I-80134 Napoli, Italy

and P. IANNELLI and A. IMMIRZI
Dipartimento di Fisica, Università di Salerno, I-84100 Salerno, Italy

(*Received 22 April 1987; accepted 1 August 1987*)

The crystal structure of this compound, a substance which exhibits smectic mesomorphism, is triclinic, $P\bar{1}$ space group, with lattice constants a = 11·280(5) Å, b = 13·598(1) Å, c = 25·650(2) Å, α = 97·85(1)°, β = 96·76(3)° and γ = 100·37(3)°. Molecules with two different conformations are present in the unit cell, and the heptyl and hexyl side-chains are extended nearly parallel to each other. The molecules are packed together in layers with their major axes inclined at 60° to the layer plane. The observed structure explains why the liquid crystal mesophases of this and related compounds are not discotic.

1. Introduction

There is increasing interest in the study of the mesogenic properties of both low molecular weight compounds and polymers. The nature and structure of the liquid crystal phases have been examined, and the relationships between molecular structure and crystal packing in ordered crystalline phases and liquid crystal properties have been studied. The acquisition of correlated observations may enable preliminary criteria to be established for the design of new molecules with mesogenic properties of the desired type.

The compound whose crystal structure is described in this paper, bis[*N*-*p*-(*n*-hexyloxy)phenyl, *p*-(*n*-heptyloxy)salicylaldiminato] copper(II) (**1**) is mesogenic. It was reported [1] among others of similar structure as yielding a discotic mesophase on the basis of both the observed morphological features of the mesophase and the supposed disc-like shape of the central core of the molecule, the latter attributed to the presumably square planar coordination around the copper atom. A further study of this compound and of some polymeric analogues containing virtually identical molecular sections has shown that the nature of the mesophase, in both the low molecular weight compounds and the polymers, is smectic rather than discotic [2].

The structural features described in this paper provide some clues as to why no molecular pile-up in columnar sets, which characterizes the typical discotic mesophase, is observed for this and related compounds.

2. Experimental

Compound (**1**) has been prepared according to the synthesis given in [1]. Crystals suitable for X-ray diffraction measurements were crystallized from chloroform/ethanol mixtures and have the shape of very thin platelets. Lattice constants and integrated intensities were measured by using a single crystal with approximate dimensions $0 \cdot 8 \times 0 \cdot 5 \times 0 \cdot 05$ mm and an Enraf-Nonius CAD4 diffractometer on-line to a PDP11/34 computer and a standard structure determination package [3].

The crystal data (Cu K_α radiation, $\lambda = 1 \cdot 5418$ Å), obtained from the scattering angles of 25 reflections, are (triclinic system): $a = 11 \cdot 280(5)$ Å, $b = 13 \cdot 598(1)$ Å, $c = 25 \cdot 650(2)$ Å, $\alpha = 97 \cdot 85(1)°$, $\beta = 96 \cdot 76(3)°$, $\gamma = 100 \cdot 37(3)°$ and $V = 3792 \cdot 7$ Å^3. The measured density D_{obs} (flotation) is $1 \cdot 05 \pm 0 \cdot 05$ g cm^{-3}, which is comparable to the $D_{calc} = 1 \cdot 16$ g cm^{-3} calculated for $Z = 3$ $C_{52}H_{72}O_6N_2Cu$ units.

Integrated X-ray diffraction intensities were measured using the conditions listed in table 1. The absorption has been corrected ($\mu = 10 \cdot 0$ cm^{-1}) according to the method described by North *et al.* [4].

Table 1. Diffraction intensity measurement.

X-ray radiation:	Ni-filtered Cu K_α
ϑ-range:	1–68°
Scan mode:	$\omega = \vartheta$
$\Delta\omega$ interval:	$1 \cdot 0 + 0 \cdot 15 \tan \vartheta°$
Prescan speed:	4·0°/min
Scan time:	selected in order to have $\sigma_I/I < 0 \cdot 1$, with a maximum of 70 s
Detector aperture:	horizontal $= 4 \cdot 50 + 0 \cdot 50 \tan \vartheta$ mm, vertical $= 4 \cdot 00$ mm
Observed decay:	< 3%
No. of reflections examined:	13224
No of reflections skipped after prescan:	3013
No. of reflections having $I < 2\sigma_I$:	2971
No. of reflections in least-squares refinement:	7240

†If $I < \sigma_I$, no further intensities are measured, and reflections are ignored in the least-squares refinement.

The full list of the observed structure factors, the fractional atomic coordinates and the complete set of interatomic distances and angles have been deposited as a Supplementary Publication, comprising 108 pages with the British Library Dorment Supply Centre. Copies may be obtained by using the procedure described at the end of this issue and by quoting SUP 16 505.

3. Structure determination and refinement

The Patterson function displays strong peaks whose positions agree with a $P\bar{1}$ distribution of heavy atoms, with one copper atom at an inversion centre (assumed to be the origin) and two copper atoms symmetrically disposed about the $(\frac{1}{2}\ \frac{1}{2}\ 0)$ position. The $P\bar{1}$ symmetry was then assumed for the whole structure, and was subsequently confirmed.

The crystal structure was determined starting from these copper atom positions and by repeated application of the Fourier method. The whole structure was obtained easily, except for twelve atoms all belonging to the methylenic side-groups in terminal positions (there are six crystallographically independent groups). By disregarding such carbon atoms, the structure was refined using the least-squares method with isotropic thermal vibration parameters for all except the copper atoms and the light atoms near copper, which were treated as anisotropic. The R-index $(\Sigma |F_{obs} - F_{calc}| / \Sigma F_{obs})$ was reduced to $0 \cdot 187$.

The difference electron density map evaluated at this stage displayed no appreciable residual density in the central part of either molecule, while in the regions lacking atoms there were scattered residual densities of the order of 2·0 e/Å^3. This indicates structural disorder in the region of the terminal atoms. Since this disorder should be of a conformational nature,we have attempted to refine this part of the structure also, using a constrained molecular model with fixed bond lengths and bond angles and free torsion angles. Starting from a canonical model with planar zigzag conformations, convergence was achieved (though with very high thermal parameters) with a significant decrease of the R-index to 0·135. The positions obtained represent, of course, only the most frequently occupied atomic positions.

All calculations were made using the Shelx package [5]. The contribution of the hydrogen atoms in the aromatic rings was also considered on the basis of the positions calculated according to the sp^2 geometry.

4. Results and discussion

The final atomic coordinates and thermal parameters are listed in table 2, and the relevant bond lengths and angles are given in table 3. The very uneven shape of the crystal and, most probably, an incompletely ordered packing of part of the flexible methylenic chains did not allow a fully satisfactory refinement of the structure to be made. None the less, all the structural features relevant to our purposes are unequivocally defined.

The two crystallographically independent molecules display different point group symmetries. One (molecule A, see figure 1) belongs exactly to the C_i point group as it lies at a crystallographic inversion centre, while the other (molecule B, see figure 1) roughly obeys C_2 symmetry. For bond lengths there are no significant differences between molecules A and B, and the observed values agree well with the crystal structure of *bis*-[*N*-phenyl-salicylaldiminato] copper(II) [6]. For bond angles only modest differences are found, except that the N–Cu–N and O–Cu–O angles, which are 180° by symmetry in molecule A, are considerably distorted in molecule B.

There are substantial differences between A and B at the conformational level.

(1) The coordination geometry is strictly square-planar in molecule A, but distorted towards a tetrahedral pattern in molecule B. This is evident from both the coordination bond angles (see table 3) and the distance of atoms from the least-squares plane (±0·34 Å).

(2) The *N*-bonded phenyl group is staggered with respect to the salicylaldiminato group in all cases. In molecule A two opposite values ±45·7°, occur, and in molecule B two angles with the same sign and reasonably close to the value for molecule A are found: 67·8° and 56·9° (the angles are evaluated by considering the best-fit planes of the phenyl ring and the salicylaldiminato group). These angles are close to the value of 64·9° found for bis-*N*-phenyl-salicylaldiminato-copper(II) [6].

(3) The conformations of the methylenic side-groups of the same kind (three independent groups of each kind) are very roughly comparable. The heptyl chains display substantially all-trans conformations in molecule B, and two anomalous angles (105° and 135°) in molecule A. The three crystallographically independent hexyl chains exhibit instead a single gauche angle. As the figures listed in table 2 show, the differences between the torsion angles grow with increasing distance from the parent phenyl rings.

Table 2. Atomic fractional coordinates and thermal parameters. The standard errors estimated from the least squares refinement are given in parentheses. The subscript A refer to molecule A (C_i symmetry), the subscripts B and B′ refer to the two halves of molecule B related approximately by C_2 symmetry. For the atom labeling, see figure 1. An asterisk indicates that constraints have been used in the refinement. Isotropic thermal factors are calculated as $\exp(-8\pi^2 U \sin^2\vartheta/\lambda^2)$, and anisotropic thermal factors as $\exp[-2\pi^2(U_{11}a^{*2}h^2 + \ldots + U_{12}a^*b^*hk + \ldots)]$.

Atom	*x*/*a*	*y*/*b*	*z*/*c*	*U*
Cu$_A$	1·0000(0)	0·0000(0)	0·0000(0)	—
O1$_A$	1·0721(8)	0·0587(6)	−0·0551(4)	—
N$_A$	0·9257(8)	0·1212(6)	0·0188(4)	—
C1$_A$	0·9177(10)	0·1885(8)	−0·0111(5)	—
C2$_A$	0·8707(11)	0·1359(8)	0·0676(5)	0.07(3)
C3$_A$	0·7487(11)	0·1502(8)	0·0641(5)	0·08(3)
C4$_A$	0·6975(11)	0·1678(8)	0·1107(5)	0·08(3)
C5$_A$	0·7608(11)	0·1695(9)	0·1593(5)	0.08(3)
C6$_A$	0·8808(12)	0·1540(9)	0·1614(6)	0·09(3)
C7$_A$	0·9336(11)	0·1361(9)	0·1161(5)	0·08(3)
O2$_A$	0·7198(8)	0·1844(7)	0·2066(4)	0·10(2)
C8$_A$	0·5948(13)	0·2010(11)	0·2023(5)	0·11(4)
C9$_A$	0·5723(17)	0·2351(12)	0·2588(6)	0·15(6)
C10$_A$	0·5860(19)	0·1556(13)	0·2944(6)	0·18(8)
C11$_A$	0·5648(25)	0·1966(16)	0·3513(7)	0·23(11)
C12$_A$	0·5567(33)	0·1108(20)	0·3850(10)	0·32(16)
C13$_A$*	0·537(13)	0·160(4)	0·447(1)	0·50(12)
C14$_A$	0·9634(11)	0·1939(9)	−0·0607(5)	0·07(3)
C15$_A$	1·0402(11)	0·1284(9)	−0·0803(5)	0·08(3)
C16$_A$	1·0784(11)	0·1388(9)	−0·1301(5)	0·08(3)
C17$_A$	1·0458(11)	0·2128(9)	−0·1570(5)	0·08(3)
C18$_A$	0·9765(11)	0·2796(9)	−0·1375(5)	0·08(3)
C19$_A$	0·9383(11)	0·2706(9)	−0·0908(5)	0·08(3)
O3$_A$	1·0768(8)	0·2228(7)	−0·2062(4)	0·10(2)
C20$_A$	1·1537(12)	0·1576(10)	−0·2280(5)	0·10(4)
C21$_A$	1·1708(14)	0·1915(12)	−0·2818(6)	0·13(5)
C22$_A$	1·2455(19)	0·1246(14)	−0·3121(7)	0·19(8)
C23$_A$	1·3193(22)	0·1875(23)	−0·3468(9)	0·40(20)
C24$_A$	1·2707(44)	0·1628(35)	−0·4055(10)	0·60(40)
C25$_A$	1·3600(33)	0·2253(34)	−0·4363(13)	0·43(24)
C26$_A$*	1·268(6)	0·272(6)	−0·481(2)	0·7(6)
Cu$_B$	0·4167(2)	0·6726(1)	−0·0146(1)	—
O1$_B$	0·3606(7)	0·7333(6)	0·0461(4)	—
N$_B$	0·5612(9)	0·7909(8)	−0.0058(5)	—
C1$_B$	0·5953(12)	0·8529(9)	0·0391(7)	—
C2$_B$	0·6253(12)	0·8113(10)	−0.0517(6)	0·09(3)
C3$_B$	0·6311(12)	0·9084(10)	−0·0671(6)	0·09(4)
C4$_B$	0·6852(12)	0·9269(11)	−0·1080(6)	0·10(4)
C5$_B$	0·7371(13)	0·8601(11)	−0·1364(6)	0·10(4)
C6$_B$	0·7335(12)	0·7622(11)	−0·1228(6)	0·10(4)
C7$_B$	0·6785(12)	0·7427(10)	−0·0791(5)	0·09(4)
O2$_B$	0·7878(9)	0·8664(8)	−0·1814(4)	0·12(3)
C8$_B$	0·7880(15)	0·9668(12)	−0·1995(6)	0·13(5)

Table 2 (*continued*).

Atom	x/a	y/b	z/c	U
C9$_B$	0·8649(17)	0·9649(14)	−0·2445(7)	0·18(8)
C10$_B$	0·8107(21)	0·8817(18)	−0·2914(8)	0·23(12)
C11$_B$	0·9122(30)	0·8478(24)	−0·3216(12)	0·37(21)
C12$_B$*	0·914(10)	0·896(7)	−0·377(4)	1·0(10)
C13$_B$*	1·035(14)	0·867(9)	−0·399(5)	1·7(12)
C14$_B$	0·5413(12)	0·8553(10)	0·0849(6)	0·09(3)
C15$_B$	0·4235(12)	0·7961(9)	0·0882(5)	0·08(3)
C16$_B$	0·3823(13)	0·8024(10)	0·1364(6)	0·09(3)
C17$_B$	0·4492(13)	0·8645(11)	0·1820(6)	0·10(4)
C18$_B$	0·5612(13)	0·9234(11)	0·1769(6)	0·10(4)
C19$_B$	0·6031(12)	0·9196(10)	0·1317(6)	0·09(3)
O3$_B$	0·4177(10)	0·8712(8)	0·2292(4)	0·13(3)
C20$_B$	0·3076(15)	0·8014(13)	0·2358(7)	0·14(6)
C21$_B$	0·3153(17)	0·8251(15)	0·2961(7)	0·19(8)
C22$_B$	0·2050(21)	0·7671(18)	0·3171(8)	0·26(12)
C23$_B$	0·2025(32)	0·8281(24)	0·3731(11)	0·37(20)
C24$_B$*	0·153(9)	0·760(3)	0·412(2)	0·9(7)
C25$_B$*	0·111(11)	0·830(4)	0·457(3)	0·3(8)
C26$_B$*	0·122(11)	0·746(6)	0·510(3)	1·6(9)
O1$_{B'}$	0·4240(7)	0·6388(6)	−0.0875(4)	0·09(6)
N$_{B'}$	0·3224(8)	0·5322(7)	−0·0118(5)	0·06(5)
C1$_{B'}$	0·3171(10)	0·4566(8)	−0·0510(6)	0·07(7)
C2$_{B'}$	0·2567(11)	0·5140(9)	0·0333(5)	0·07(3)
C3$_{B'}$	0·1335(11)	0·4611(9)	0·0206(5)	0·08(3)
C4$_{B'}$	0·0700(12)	0·4434(9)	0·0624(5)	0·09(3)
C5$_{B'}$	0·1212(12)	0·4750(9)	0·1136(5)	0·08(3)
C6$_{B'}$	0·2460(11)	0·5262(9)	0·1255(5)	0·08(3)
C7$_{B'}$	0·3081(11)	0·5434(8)	0·0851(5)	0·07(3)
O2$_{B'}$	0·0676(8)	0·4660(7)	0·1581(4)	0·10(2)
C8$_{B'}$	−0·0687(14)	0·4315(11)	0·1471(6)	0·12(5)
C9$_{B'}$	−0·1038(19)	0·4185(12)	0·2016(6)	0·17(7)
C10$_{B'}$	−0·0940(22)	0·5194(13)	0·2384(7)	0·20(9)
C11$_{B'}$	−0·1128(28)	0·4903(17)	0·2940(8)	0·26(13)
C12$_{B'}$*	−0·180(11)	0·565(4)	0·325(2)	0·8(8)
C13$_{B'}$*	−0·167(10)	0·539(5)	0·383(2)	0·8(7)
C14$_{B'}$	0·3646(11)	0·4581(9)	−0·0989(5)	0·07(3)
C15$_{B'}$	0·4157(11)	0·5492(10)	−0·1135(5)	0·08(3)
C16$_{B'}$	0·4610(11)	0·5415(10)	−0·1646(5)	0·09(3)
C17$_{B'}$	0·4573(13)	0·4477(11)	−0·1928(6)	0·10(4)
C18$_{B'}$	0·4048(12)	0·3600(10)	−0·1759(6)	0·09(3)
C19$_{B'}$	0·3600(11)	0·3657(10)	−0·1311(5)	0·08(3)
O3$_{B'}$	0·5047(9)	0·4340(8)	−0·2398(4)	0·12(3)
C20$_{B'}$	0·5650(17)	0·5275(14)	−0·2555(8)	0·15(6)
C21$_{B'}$	0·5984(27)	0·4755(15)	−0·3069(9)	0·25(13)
C22$_{B'}$	0·6571(34)	0·5540(19)	−0·3389(11)	0·36(19)
C23$_{B'}$	0·6648(51)	0·4963(26)	−0·3944(12)	0·47(31)
C24$_{B'}$*	0·746(12)	0·569(4)	−0·425(2)	1·2(11)
C25$_{B'}$*	0·696(13)	0·485(6)	−0·4960(4)	0·6(9)
C26$_{B'}$*	0·826(17)	0·597(9)	−0·510(4)	2·3(12)

Table 2 (*continued*).

	Anisotropic thermal parameters					
	U_{11}	U_{22}	U_{33}	U_{23}	U_{13}	U_{12}
Cu_A	0·075(2)	0·063(1)	0·115(2)	0·031(1)	0·024(2)	0·025(1)
$O1_A$	0·101(6)	0·079(5)	0·147(9)	0·057(6)	0·048(6)	0·044(5)
N_A	0·072(6)	0·051(5)	0·113(9)	0·026(6)	−0·007(6)	0·011(4)
Cl_A	0·075(7)	0·051(6)	0·095(9)	0·011(6)	0·010(7)	0·018(5)
Cu_B	0·063(1)	0·052(1)	0·141(2)	0·017(1)	0·010(1)	0·007(1)
$O1_B$	0·074(5)	0·071(5)	0·119(8)	0·005(5)	0·013(5)	0·018(4)
N_B	0·073(7)	0·059(6)	0·145(10)	0·024(7)	0·014(7)	0·018(5)
Cl_B	0·077(9)	0·042(6)	0·159(15)	0·013(8)	−0·013(9)	0·004(6)
$O1_{B'}$	0·089(6)	0·059(5)	0·129(8)	0·013(5)	0·022(5)	0·009(4)
$N_{B'}$	0·062(6)	0·056(6)	0·120(9)	0·020(6)	0·006(6)	0·014(4)
$Cl_{B'}$	0·069(8)	0·044(6)	0·139(13)	0·008(7)	−0·004(8)	0·014(5)

Table 3. Relevant bond distances (in Å), bond angles (in degrees) and torsion angles (in degrees). Estimated standard errors are in parentheses. The average standard error for torsion angles is ~ 1°. Column A refers to molecule A; columns B and B′ to the two halves of molecule B related to each other by approximate C_2 symmetry.

	A	B	B′
Bond distances			
Cu–O	1·908(10)	1·891(9)	1·876(10)
Cu–N	2·007(10)	2·042(9)	2·026(9)
O–C15	1·30(2)	1·32(2)	1·29(2)
C15–C14	1·43(2)	1·44(2)	1·39(2)
C14–C1	1·43(2)	1·38(2)	1·40(2)
C1–N	1·28(2)	1·30(2)	1·32(2)
N–C2	1·47(2)	1·48(2)	1·47(2)
Bond angles			
N–Cu–O	91·3(4)	90·9(4)	91·9(4)
N–Cu–O′	88·7(4)	92·0(5)	93·8(4)
Cu–O–C15	128·7(9)	129·1(8)	126·6(9)
Cu–N–C1	123·5(9)	121·0(11)	120·4(9)
N1–Cu–N1′	180	159·1(4)	159·1(4)
O1–Cu–O1′	180	156·3(4)	156·3(4)
Torsion angles			
C1–N–C2–C3	52	−55	−48
Cu–N–C2–C7	55	−58	−50
C16–C17–O2–C20	−5	5	3
C17–O2–C20–C21	−179	173	−179
O2–C20–C21–C22	−177	176	175
C20–C21–C22–C23	−149	−159	−169
C21–C22–C23–C24	−106	−148	−170
C22–C23–C24–C25	−175	−160	−165
C23–C24–C25–C26	−135	−157	−175
C4–C5–O1–C8	−1	−10	−10
C5–O1–C8–C9	−170	171	175
O1–C8–C9–C10	−61	63	73
C8–C9–C10–C11	179	−152	−171
C9–C10–C11–C12	170	−104	−146
C10–C11–C12–C13	179	172	−169

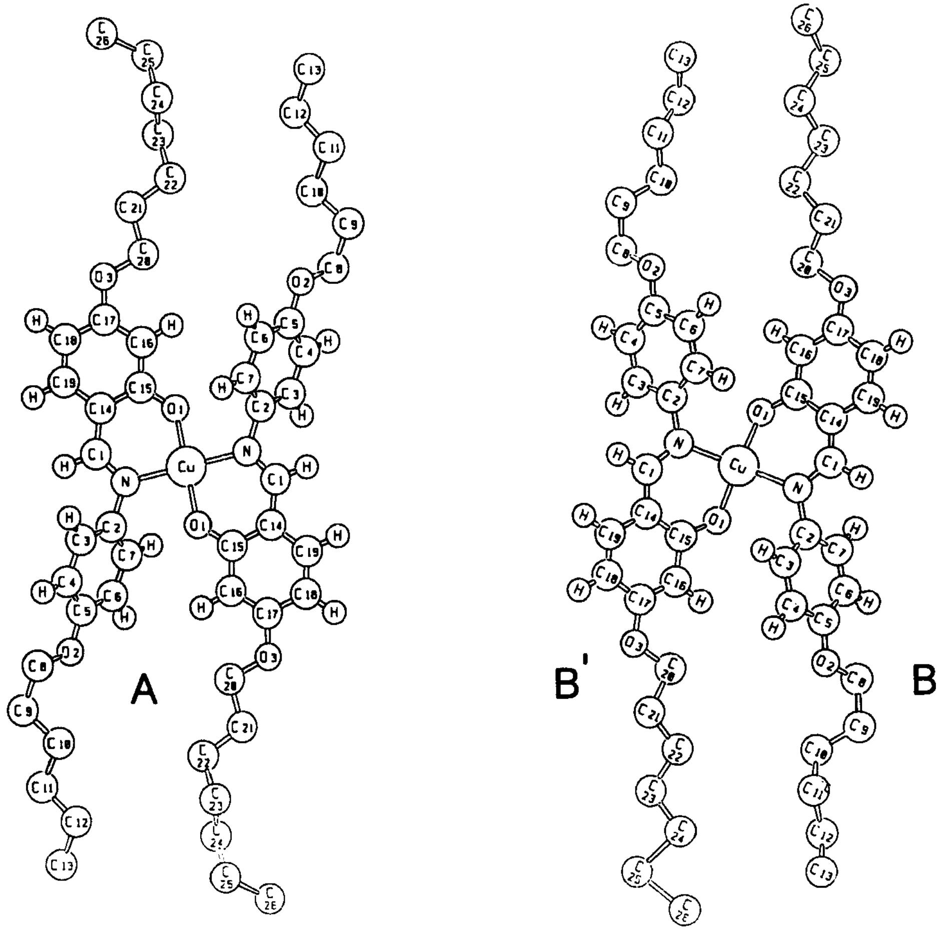

Figure 1. Structure of molecules A and B.

Since no particularly close intramolecular interaction is active, the presence of two different molecular conformations in the same crystalline phase suggests that the packing forces are the only driving force for the co-crystallization of different conformers.

Although some conformational angles differ from 180° in the methylenic side-groups, both types of molecule occur in an almost completely elongated form, with the flexible chains roughly parallel to each other. The molecular shape may be approximated by a prism with edges of about 30, 10 and 6 Å (including van der Waals radii). Molecules of both types (A and B) are packed togethr in layers parallel to the crystallographic xy plane, with their elongation axes paralel to each other and tilted by about 60° with respect to the layer plane (see figure 2; the elongation axis has been defined as the direction of the major axis of the central ellipsoid of inertia of the molecule, considering atoms of unit mass and neglecting hydrogen atoms). This arrangement may be seen as a pro-smectic structure consistent with the smectic nature of the liquid crystal phases actually occurring. In fact the compound melts to give a smectic C phase (i.e. a layered structure with the director tilted with respect to the

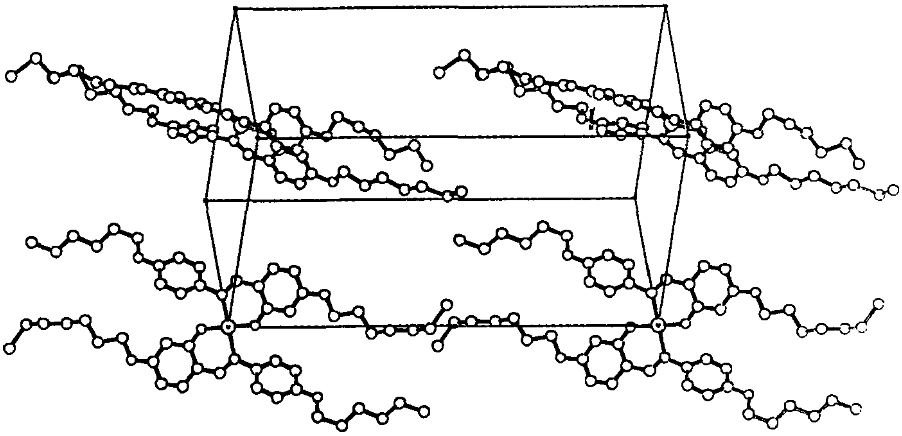

Figure 2. Prosmectic packing of molecules A and B in layers parallel to the crystallographic *xy* plane. For clarity, only some molecules are shown.

layer axis) that transforms, at 428 K, into a smectic A phase (with the director parallel to the layer axis) whose smectic periodicity was measured at 433 K to be 26·1 Å [2].

The molecular structure that has been found, although strictly referring to a crystal phase, provides some clues to the absence of discotic mesomorphism. The formation of a cylindrical pile of molecules having flexible tails arranged with twofold symmetry, requires their packing to be close but rotationally disordered around the cylinder axis. The considerable rotation of the phenyl groups with respect to the salycilaldiminato–copper groups, that leads to an uneven increase in the thickness of the molecular cores, appears to be the major obstacle to the formation of discotic packing.

References

[1] Ovchinnikov, I. V., Galayametdinov, Yu. G., Ivanova, G. I., and Yagfarova, L. M., 1984, *Dokl. Akad. Nauk SSSR*, **276**, 126.

[2] Carfagna, C., Caruso, U., Roviello, A., and Sirigu, A., 1987, *Makromolec. Chem. rap. Commun.*, **8**, 345.

[3] *CAD4 Operation Manual*, 1977 (Enraf-Nonius).

[4] North, A. C. T., Phillips, D. C., and Mathews, F. S., 1968, *Acta crystallogr.* A, **24**, 351.

[5] Sheldrick, G., 1977, Shelx-76: program for crystal structure determination, University Chemical Laboratory, Cambridge.

[6] Wei, L., Stogsdill, R. M., and Lingafelter, E. C., 1964, *Acta crystallogr.*, **17**, 1058.